ACCOUNTS
of chemical research

Relaxation-Assisted Two-Dimensional Infrared (RA 2DIR) Method: Accessing Distances over 10 Å and Measuring Bond Connectivity Patterns

IGOR V. RUBTSOV
Department of Chemistry, Tulane University, New Orleans, Louisiana 70118

RECEIVED ON JANUARY 10, 2009

CONSPECTUS

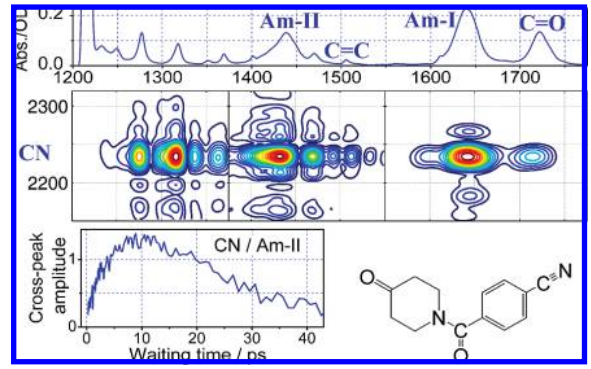

Development of new approaches for measuring three-dimensional structures and dynamics of structural changes is important for a number of natural sciences, including structural biology, where it can lead to understanding the physical bases of molecular recognition and catalysis. A two-dimensional infrared (2DIR) spectroscopy method permits measuring pairwise interactions among vibrational modes in molecules providing a molecular scale ruler for delivering structural constraints, such as the distances between the vibrational modes, angles between their transition dipoles, and the energy-transfer rates between them. While there is a large variety of systems that have recently been interrogated using 2DIR, questions remain of how to measure structural features of larger molecules. The challenges of working with larger molecules, such as proteins, include very congested vibrational spectra, a small range of distances accessible by the 2DIR method, and sensitivity issues. This Account describes the efforts of our laboratory to overcome some of these challenges.

First, we discuss the dual-frequency 2DIR approach, which provides the highest selectivity to a particular pair of vibrational reporters and highest sensitivity. Second, we describe our steps in developing vibrational labels, novel for 2DIR, such as C≡N and C−D stretching modes that have frequencies in the water transparency region, as well as the modes in the fingerprint region. The schemes suitable for labeling amino acids are discussed.

Next, we describe the novel relaxation-assisted 2DIR (RA 2DIR) method, developed in our laboratory. The method uses vibrational relaxation and vibrational energy transport in molecules and the thermalization process on a molecular scale, to generate stronger cross-peaks. An 18-fold cross-peak amplification was observed for the modes separated by about 11 Å using the RA 2DIR method, and larger amplifications are expected for larger distances between the modes. Large amplification provided by the RA 2DIR method enhances the sensitivity of 2DIR spectroscopy and permits longer range structural measurements. In addition to generating stronger cross-peaks, a correlation of the energy transport time with the intermode distance is demonstrated. This correlation permits measurements of mode-connectivity patterns in molecules much similar to those available in total correlation spectroscopy (TOCSY) and heteronuclear multiple-bond correlation (HMBC) methods of 2D nuclear magnetic resonance (NMR) spectroscopy. It is our hope that, with a proper calibration, the RA 2DIR method will permit speedy assessments of distances and the bond connectivity patterns in molecules and reach the level of an analytical method.

1. Introduction

Two-dimensional infrared (2DIR) spectroscopy, introduced a decade ago,[1−3] is developing into a widely used method for measuring structures of molecules in solution at physiological temperatures. The 2DIR method can also access dynamics of structural changes occurring on a variety of time scales ranging from tens of femtoseconds to seconds, revealing equilibrium[4,5] and non-equilibrium dynamics.[6,7] Structural measurements using

Published on the Web 05/22/2009 www.pubs.acs.org
10.1021/ar900008p CCC: $71.50

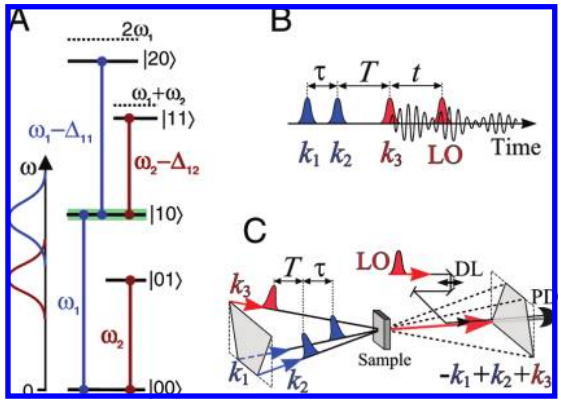

FIGURE 1. (A) Energy diagram for two vibrational modes showing one- and two-quantum states. Spectra of IR pulses suitable for dual-frequency (DF) 2DIR are shown (left). (B) Delays between the pulses in DF 2DIR measurements. (C) Phase-matching beam geometry for DF 2DIR ($k_1 > k_3$).[16]

2DIR have been performed on a variety of molecular systems, such as peptides,[1,8,9] relatively small compounds, and solvents.[4,10,11]

The 2DIR spectroscopy has many varieties (see ref 12 and references therein), but most importantly, it can measure a pairwise interaction (coupling) of vibrational modes (ω_1 and ω_2) in a molecule, which is manifested in a shift of the combination band level for the two modes, Δ_{12}, called an off-diagonal anharmonicity (Figure 1A). The off-diagonal anharmonicity can be experimentally measured and linked to the distance between the interacting modes using theoretical modeling.[13] Other structural reporters, such as the angles between transition dipoles of the modes and the energy-transfer rates between the modes, can be obtained from the cross-peak measurements.[12] While 2DIR spectroscopy in general has been applied to systems of various complexity, including proteins,[1,8] the 2DIR measurements with clear *cross-peak* specificity were only reported for smaller molecular systems. Application of 2DIR cross-peak measurements to study protein structures and dynamics can lead to an understanding of the correlation between their structure and functioning. The experimental challenges in applying 2DIR methods for measuring structural features in proteins are associated with the complexity and congestion of their vibrational absorption spectra, which result in difficulties of extracting structural constraints from the measurements.

In this Account, we summarize ongoing efforts in the laboratory to further develop multidimensional IR (MDIR) spectroscopy toward making it suitable for cross-peak measurements in larger molecules. We first overview the dual-frequency 2DIR method, which, although proposed over 5 years ago,[14] has not yet received wide popularity. Next, we describe novel labeling strategies, including those suitable for targeting larger molecules and biopolymers. Then, we introduce the relaxation-assisted 2DIR (RA 2DIR) method,[15,16] designed in our laboratory and demonstrate its advantages and applications.

2. Dual-Frequency 2DIR

Early 2DIR measurements were performed using a "single-spectrum" style, where all IR pulses needed for the measurements were obtained by splitting a single laser beam into a required number of parts.[1,2,17] Because of a common origin, all of the pulses have the same spectrum, with the width dependent upon the pulse duration; a typical width was 150−200 cm^{-1} (*fwhm*), although much shorter pulses with the spectral width exceeding 400 cm^{-1} were also generated.[10] Therefore, the modes that could be interrogated using a "single-spectrum" 2DIR have to be close in frequency. Practically, it means that mostly the modes of the same type but separated in frequency were used. Occasionally modes of different type could be excited by the pulse of ca. 200 cm^{-1} width, as in the case of amide-I and amide-II (Am-I and Am-II) transitions.[18] Note that, while shorter IR pulses allow for resolving faster processes and interrogate broader transitions, their use for measuring cross-peaks involving narrow vibrational transitions is excessive; the broader spectrum has a smaller spectral density at particular frequencies of absorption, resulting in smaller excitation probability and weaker 2DIR cross-peaks.

Development of dual-frequency 2DIR, particularly the heterodyned photon-echo (HPE) 2DIR,[14,19,20] permitted exciting transitions of very different frequencies, which immensely increased the range of cross-peaks accessible via 2DIR. To perform such measurements, two independently tunable mid-IR pulses were generated at the same time (Figure 1C). Each beam was split into two parts; three beams were focused onto the sample, and the forth beam was used for heterodyning as a local oscillator (LO) (panels B and C of Figure 1). The diagonal peaks, requiring IR pulses of the same frequency, are suppressed or completely eliminated in the DF 2DIR scheme, and the spectrum can be focused solely on the cross-peaks of interest. The 2DIR spectrum of 3-cyanocoumarin illustrates advantages of the DF 2DIR approach (Figure 2).[20] The spectrum of the k_1 and k_2 pulses (left panel) was centered at the C≡N mode frequency, while the k_3 and LO spectrum was centered at the C═O frequency (top panels). As a result, the CN−CO cross-peak dominates the spectrum. Note that, despite about 500 cm^{-1} separation between the CN and CO mode frequencies, the diagonal CO peak appears in the spectrum. It

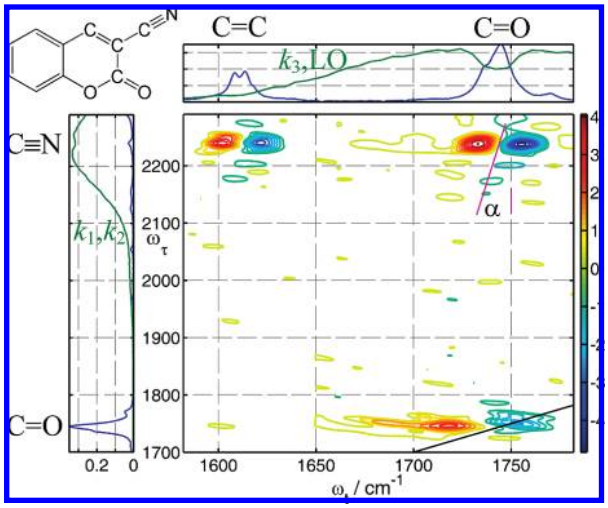

FIGURE 2. Dual-frequency 2DIR absorptive spectrum of 3-cyanocoumarin measured at $T = 0.67$ ps.[20] Attached panels (here and for other 2DIR spectra) show the linear absorption spectrum (blue) and the spectra of the IR pulses (green).

would, however, be ca. 500 times stronger if the k_1 and k_2 pulse spectrum were also centered at the CO frequency. Such strong suppression of the diagonal features leads to a larger dynamic range and higher sensitivity for measuring weaker cross-peaks using DF 2DIR.

Because the IR pulses for DF 2DIR are generated independently, they are not necessarily phase-locked. Experimental conditions with phase locking of all pulses[14] or pairwise phase locking were tested.[19] In this Account, we focus on the pulse sequences that require only pairwise phase locking (Figure 1B). The DF 2DIR method, which is similar to heteronuclear 2D nuclear magnetic resonance (NMR), permits using *any* vibrational mode as a structural label, given that laser pulses can be generated at such frequencies.

3. IR Reporters for 2DIR Spectroscopy

Vibrational absorption spectra (linear spectra) of molecules with less than 30 atoms are often simple enough so that some of the existing vibrational modes in the molecule can serve as labels for the 2DIR measurements. Vibrational spectra of large molecules are complex and congested, making the use of vibrational labels essential. A "good" vibrational label should have a spectrally resolved transition in a part of the spectrum that is free of other transitions of the molecule and the solvent and should have a reasonably large extinction coefficient. It is also advantageous to have a localized mode as a label (the mode with only a few atoms moving) because it simplifies the analysis and permits measuring atom-sensitive structural constraints.

Stretching modes with a large transition dipole (strong IR modes), such as C═O, Am-I, Am-II, O−H, and N−H, are often used in 2DIR measurements. These modes, however, are highly abundant in biopolymers and/or solvent, which complicate their use as structural reporters. The necessity in providing vibrational labels has been realized very early in the development of 2DIR spectroscopy.[17] Isotope substitutions provide least perturbing labels; isotopic substitutions in amides, $^{13}C^{16}O$ and $^{13}C^{18}O$, shift the frequency of the Am-I mode by ca. 40 and 64 cm^{-1}, respectively.[21] Such labeling has been shown to work well for a number of peptides of up to about 30 amino acids.[9] It is not clear if the 64 cm^{-1} shift is sufficient for spectrally isolating the mode in proteins because they have very broad Am-I bands and other modes of commensurate frequencies.

C−D Stretching Modes. Another readily accessible isotope substitution is the hydrogen−deuterium substitution. The protons on OH or NH groups are generally exchangeable in protic solvent, and their labeling with deuterium in organic molecules is less convenient. Several research groups used OD and ND for studying dynamics of solvents, water and alcohols,[10] or accessing structures of organic molecules in aprotic solvents.[22]

In contrast, covalent carbon−deuterium (C−D) bonds are not exchangeable and also absorb in an otherwise transparent region of the protein IR spectrum. The challenge of accessing covalent C−D groups via 2DIR is associated with their small-transition dipoles. Nevertheless, CD labels have been used in linear IR spectroscopy in small molecules, and recently, they have been site-selectively incorporated into proteins reporting on folding with high structural and temporal resolution.[23] Despite small extinction coefficients of CD modes, the cross-peaks were measured between the C−D and C≡N modes in acetonitrile-d_3, where the extinction coefficient of the symmetric CD_3 stretching mode is ca. 1 M^{-1}cm^{-1} (Figure 3),[15,24] or between the C−D and C═O modes in formamide-d_3[25] and benzaldehyde-d_6 (Figure 4).[15]

More recently, leucine amino acid with a perdeuterated side chain (Leu-d_{10}, Figure 5A) has been introduced as a structural label.[26,27] The exciton interaction of the 10 CD stretching transitions of Leu-d_{10} results in the formation of reasonably strong absorption peaks around 2050−2220 cm^{-1}, featuring extinction coefficients of up to 120 M^{-1} cm^{-1} (Figure 5C). The CD transitions of Leu-d_{10} were characterized using anharmonic density functional theory (DFT) computations (Figure 5C) and the RA 2DIR measurements (*vide infra*). The CD−Am-I, CD−CO (Figure 5B), and CD−Am-II cross-peaks in Leu-d_{10}-Boc

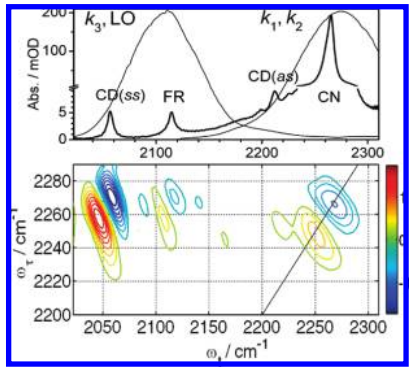

FIGURE 3. Dual-frequency 2DIR nonrephasing spectrum (lower panel) of deuterated acetonitrile (CD_3CN) in chloroform measured at $T = 0.6$ ps.[15,24]

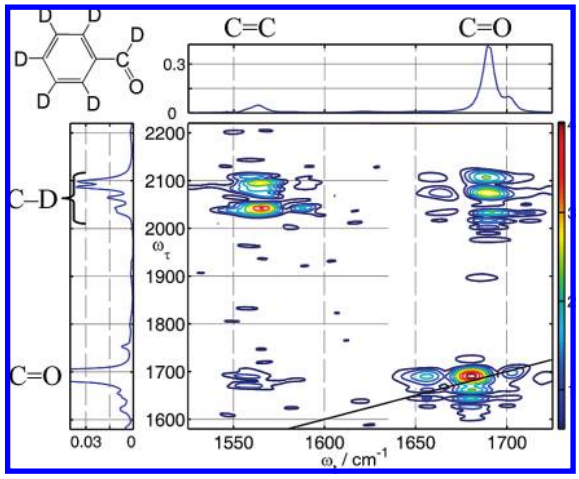

FIGURE 4. Dual-frequency 2DIR absolute-value spectrum of perdeuterated benzaldehyde measured at $T = 0.6$ ps.

were measured, demonstrating a strong potential of CD labeling for structural studies in proteins.

Modes in the Fingerprint Region and Other Labels. Several other labels with frequencies in the water transparency (and weak molecular absorption) region from 2000−2600 cm^{-1} have been introduced. The cyano group offers the stretching mode at 2345−2365 cm^{-1} with a respectable extinction coefficient of ca. 50 M^{-1} cm^{-1}.[20,28] The cross-peaks originated from interactions of C≡N modes with C═O and C═C modes provide convenient structural handles, as demonstrated for 3-cyanocoumarin (Figure 2); the anharmonic shifts here are sufficiently large, 2.0 and 12 cm^{-1}, respectively, because of a spatial closeness of the interacting modes.[20] Other promising IR labels include the S−H stretching mode of cysteine (~2550 cm^{-1}), useful if located in a hydrophobic environment,[29] and extremely strong stretching modes of asides, −N═N═N.[30]

The fingerprint region, 900−1500 cm^{-1}, bears many vibrational modes specific for a particular molecule, thus providing wide opportunities for structural measurements. Despite

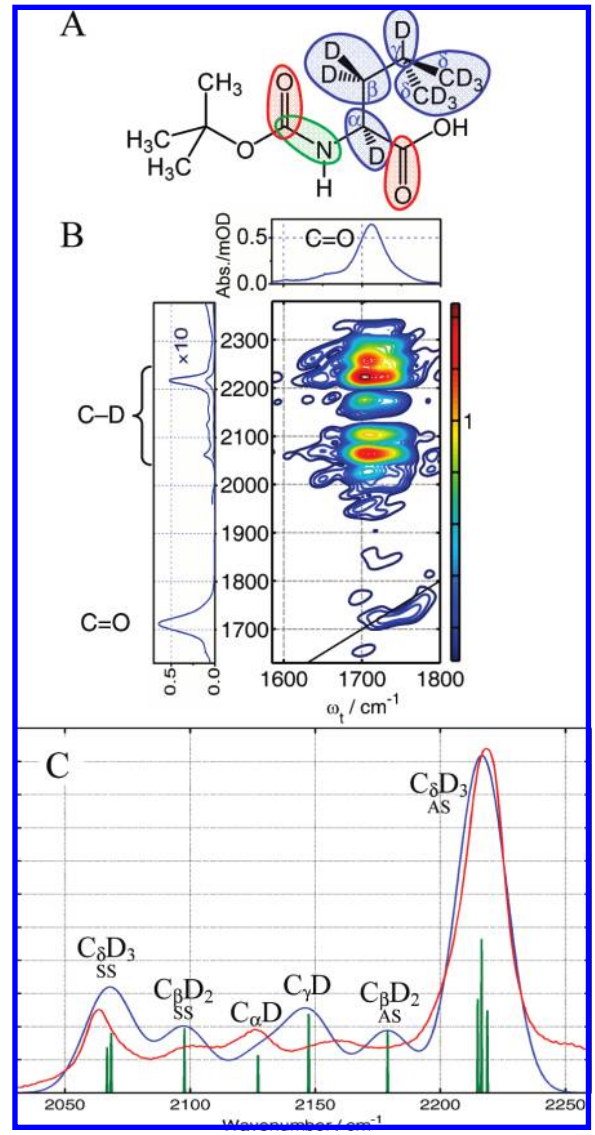

FIGURE 5. (A) Structure, (B) dual-frequency 2DIR rephasing absolute-value spectrum measured at $T = 3.0$ ps,[26,27] and (C) absorption spectrum (red) of Leu-d_{10}-Boc in chloroform. The *an*harmonic line spectrum (green), computed using the DFT method with B3LYP functional and 3-21G basis set, and modeled spectrum (blue), obtained by broadening of the line spectrum, are shown in C. No frequency scaling applied.

the difficulty of assigning the modes and delocalized character of many of the modes in this region, the fingerprint region is very attractive for the DF 2DIR measurements.[31] There are many modes contributing to the fingerprint region, including C−C, C−O−C, C−C−O, and C−N stretches, CH, CH_2, and CH_3 rocking, waging, scissoring, etc. Figure 6 shows numerous cross-peaks between high-frequency modes and the modes in the fingerprint region for PBN.[32] The S═O stretching mode in sulfoxides has recently been implemented as structural reporters.[31]

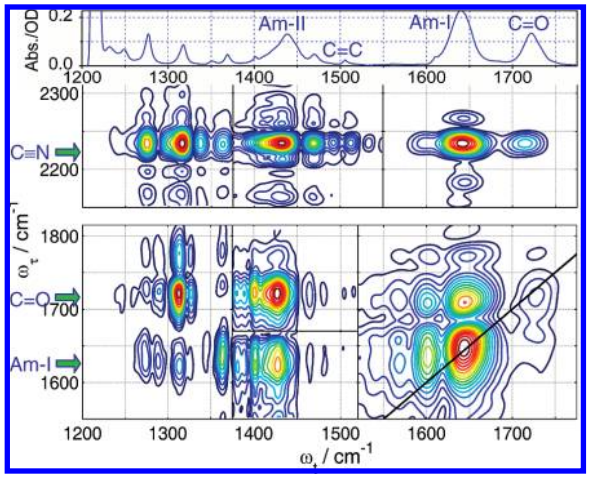

FIGURE 6. Dual-frequency RA 2DIR rephasing absolute-value spectrum of PBN measured at $T = 10$ ps.[32]

Because of small-transition dipoles, many convenient labels are not easy targets with 2DIR. Nevertheless, if the intermode distance is small enough (the modes overlap), the coupling is substantial because of a mechanical contribution. As the distance between the probed modes increases, the direct coupling strength falls rapidly,[16] which may render weak IR labels inefficient for the 2DIR measurements over larger distances. A new approach has recently been proposed, the RA 2DIR method, which increases the range of distances accessible via 2DIR.[16]

4. RA 2DIR: The Way of Enhancing the Range of Accessible Distances

Principles of RA 2DIR. The RA 2DIR method relies on two main ideas. First, the modes excited by a short laser pulse relax rapidly, and the excess energy must propagate in the molecule as a part of the energy dissipation process that leads to thermal equilibration. Second, the intermode coupling is substantial when the modes have a large spatial overlap. For the modes with large transition dipoles, the electric, through-space, coupling could be dominant,[17] while weak IR modes interact through bond, mechanically.[33]

RA 2DIR relies on relaxation in a vibrationally excited molecule followed by a transport of the excess energy in the direction of the "probed" mode. The excess energy propagates in the molecule, exciting various modes, and reaches the site of the molecule where the "probed" mode is located, exciting other modes, X, around it (Figure 7B). Some of these modes, X, are coupled strongly to the "probed" mode because of a strong spatial overlap with it. If such a mode is populated via energy transport from the initially excited mode, a cross-peak will appear in the 2DIR spectrum (Figure 7E), roughly at the same frequencies as the direct-coupling cross-peaks. More accurately, the real part 2DIR spectrum will show two peaks at (ω_2, ω_1) and (ω_2, $\omega_1-\Delta_{X2}$), having different signs (Figure 7E), which are often seen as a single peak in the absolute-value spectra. A clear switch of the cross-peak character from the direct coupling (described by $\Delta_{CN/CO}$, Figure 8A) to the relaxation assisted (described by $\Delta_{X/CO}$, Figure 8C) has been demonstrated in 3-cyanocoumarin by following the waiting-time evolution of the cross-peak position.[16] The RA 2DIR method has similarities with the homonuclear total-correlation spectroscopy (TOCSY) 2D NMR method and its heteronuclear counterpart, heteronuclear multiple-bond correlation (HMBC).

What are the advantages of RA 2DIR? Clearly, the RA 2DIR cross-peak amplitude does not reflect the direct interaction among ω_1 and ω_2 modes, which, in traditional 2DIR, is linked to the distance between the vibrating groups. However, the method can provide significant amplification of the cross-peak amplitude, especially for the modes separated by a substantial distance. The amplitude of the RA 2DIR cross-peak depends upon two main factors: the coupling strength of the ω_2 and ω_X modes, which results in a shift of the (2 + X) combination band, Δ_{X2} (Figure 7D), and the occupation number (that is the excited-state population) for the X mode(s), achieved via the energy transport. If $\Delta_{X2} \gg \Delta_{12}$, the relaxation-assisted cross-peaks could be stronger than the direct-coupling cross-peaks, despite small occupation numbers for the X modes. Also, the pace of energy transport may report on the distance between the initially excited and probed modes. We will next illustrate new structural constraints accessible with RA 2DIR.

Cross-Peak Amplification. Because of the small distance between the CN and CO groups in 3-cyanocoumarin (~3.1 Å), no increase of the CN/CO cross-peak amplitude was observed.[15,16] In 4-acetylbenzonitrile, however, the CN−CO distance is about twice as big (~6.5 Å) and a 6-fold increase in the cross-peak amplitude was detected because of the appearance of the relaxation-assisted cross-peaks (Figure 9).[16] The maximum is observed at the waiting time of 12 ps, the time required for the excess energy to reach the CO site of the molecule, referred to as the (energy) arrival time, T_{max}. The decay of the cross-peak amplitude seen at $T > T_{max}$ reflects the cooling process, i.e., continuing energy equilibration in the molecule toward a more uniform distribution and the energy dissipation to the solvent. The lifetime of the initially excited mode (CN in these examples) clearly affects the T_{max} values, providing a delay for the start of the energy transport. These experiments have shown a potential of RA 2DIR to increase substantially the range of accessible distances.

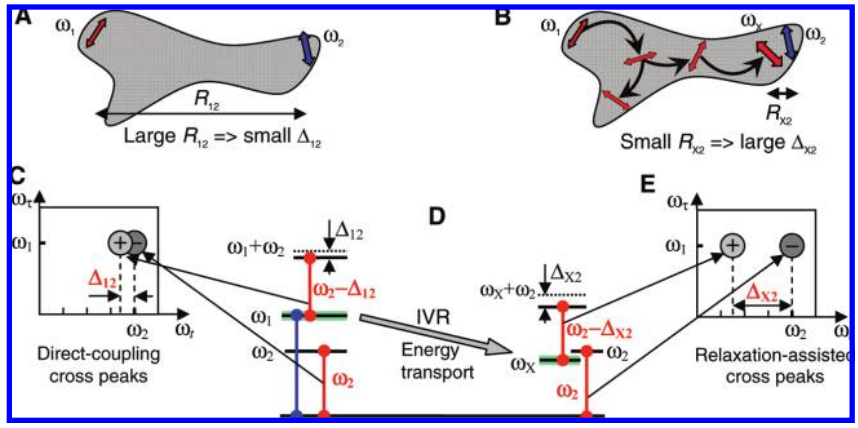

FIGURE 7. Cartoons (A and B) and 2DIR spectra (C and E) illustrating the direct-coupling and relaxation-assisted cross-peaks, respectively, and the energy diagram (D).

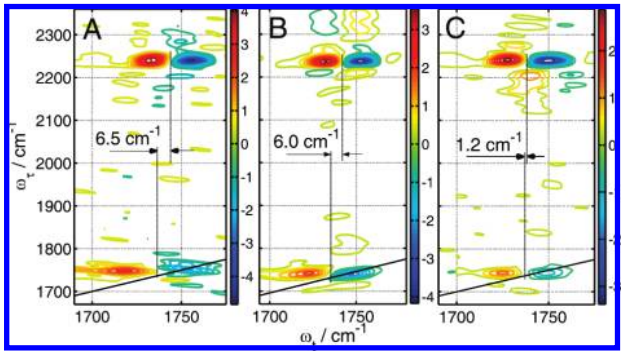

FIGURE 8. 2DIR absorptive spectra of 3-cyanocoumarin in dichloromethane measured at waiting times of (A) 0.670 ps, (B) 2 ps, and (C) 4 ps.[16]

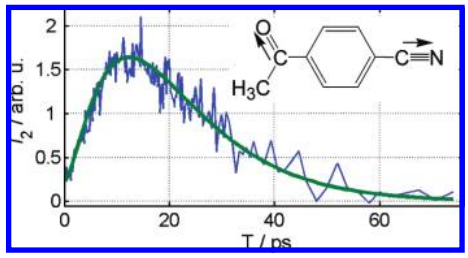

FIGURE 9. Waiting-time dependence of the CN/CO cross-peak amplitude for 4-acetylbenzonitrile.[16]

A much larger amplification factor (γ), the ratio of the cross-peak amplitude at the maximum to that at $T = 0$, has been demonstrated in PBN (Figure 10A). Figure 10B shows the waiting-time dependences of the CN/Am-I and CN/CO cross-peak amplitudes,[32] which demonstrate the amplification factors of 4.3 ± 0.6 and 18 ± 2, respectively. Such strong amplification made it easy to detect the cross-peak between the CN and CO modes regardless of the large spatial separation of the groups (~11 Å). Slight tuning of the k_3 spectrum to center at the CO frequency resulted in the RA 2DIR spectrum dominated by the CN/CO cross-peak (panels C and D of Figure 10), emphasizing the power of the dual-frequency approach.

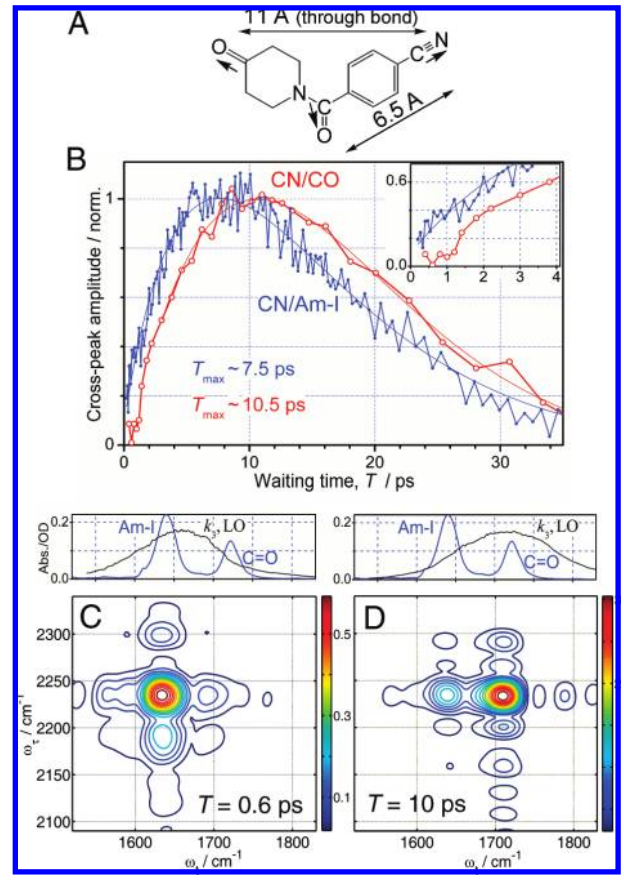

FIGURE 10. (A) Structure of 4-(4-oxo-piperidine-1-carbonyl)-benzonitrile (PBN). (B) Normalized amplitudes of the CN/Am-I (blue) and CN/CO (red) cross-peaks as a function of the waiting time. Graphs C and D show the absolute-value rephasing 2DIR spectra of PBN measured at T of 0.6 and 10 ps, respectively.[32]

The origin of the large amplification factors observed using RA 2DIR is in a softer distance dependence for the energy transport efficiency compared to that of the direct coupling. The direct-coupling distance dependence varies with the coupling mechanism. The electric point-dipole−point-dipole through-space coupling decays with distance as a square of

the transition dipole−dipole interaction energy, resulting in $1/R^6$ distance dependence for Δ_{12}.[17] The distance dependence of the mechanical coupling is less understood. It strongly depends upon the structure of the bridging groups separating the two modes, particularly on the type of bonds and mode frequencies at the bridge. Exponential decay with distance is expected for Δ_{12} when the frequencies at the bridge are far from the frequencies of the two modes. In a simplest model, the RA cross-peak amplitude can be associated with the amount of excess energy delivered to the ω_2 site from the ω_1 mode (Figure 7B). The maximum cross-peak amplitude will be achieved when the excess energy at the ω_2 site reaches a maximum. The assumption that the energy transport on a molecular scale can be treated as heat conduction in macro objects leads to $1/R$ and $1/R^2$ dependences for the maximal temperature reached at distance R from the heat source for one- and two-dimensional cases, respectively. Such a drastic difference in distance dependences for the direct-coupling and relaxation-assisted cross-peaks suggests that larger amplification factors should be seen for larger distances between the modes.

Correlating the Arrival Time with the Intermode Distance. Does the arrival time correlate with the distance? One could imagine that the excited high-frequency mode relaxes into largely delocalized modes, so that there would be no difference in the arrival times for the "probed" modes at different distances from the initially excited mode. In fact, there are many low-frequency modes that are delocalized over the whole molecule, such as the bending and rocking motions of the whole structure. The experiments, however, demonstrate quite a different effect.

The arrival time for the CN/Am-I cross-peak in PBN, 7.5 ± 0.7 ps, was found to be smaller than that for the CN/CO cross-peak, 10.6 ± 0.6 ps (Figure 10B), indicating directly the presence of a monotonic correlation of the arrival times with the intermode distance. Interestingly, the amplification factor also correlates with distance; as expected, γ is larger for larger intermode distances.

RA 2DIR cross-peaks were measured in PBN for many modes in the fingerprint region with initial excitation of the CN, CO, and Am-I modes;[32] the RA 2DIR spectrum shows over 25 cross-peaks involving 11 vibrational modes (Figure 6). The dependences of the cross-peak amplitudes on the waiting time have been measured for most of the cross-peaks seen in Figure 6. Thick gray horizontal lines in Figure 11 symbolize the molecular skeleton of PBN. The arrival times are shown by the arrows starting from the group where the initially excited mode is located. For example, the top scheme shows the

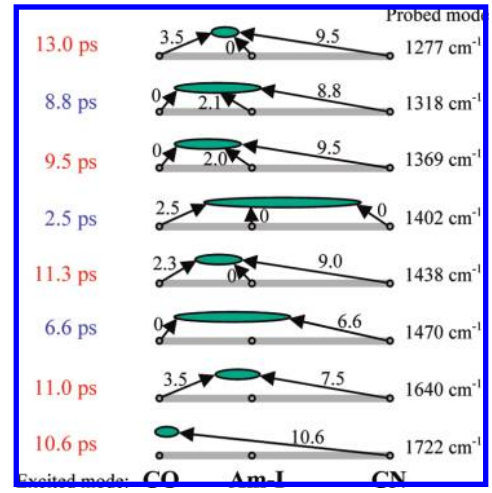

FIGURE 11. Summary of the arrival times, given in picoseconds above the arrows, measured in PBN (see the text). The arrows start at three initially excited modes, CN, Am-I, and CO, and indicate the energy transport to the probed mode indicated on the right side of each diagram. The number on the left side of each diagram is the sum of the arrival times for each probed mode when the CN and CO modes were excited.[32]

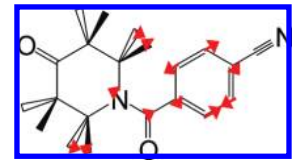

FIGURE 12. Atom displacements of the normal mode in PBN assigned to the peak at 1402 cm^{-1}.[32]

arrival times for the mode at 1277 cm^{-1}, when the CO, Am-I, or CN modes were initially excited; the corresponding arrival times for the CO/1277, Am-I/1277, and CN/1277 cross-peaks are 3.5, 0 (no rise), and 9.5 ps, respectively. The number at the left of each scheme is the sum of two arrival times from the CN and CO modes to a given probed mode, which can be associated with the total time required for energy to cross the molecule. Approximate additivity for the total time is observed for many modes, especially for the well-characterized and localized modes, such as CO, Am-I, and Am-II. The additivity confirms that the arrival time correlates with the intermode distance, bringing an opportunity of using the RA 2DIR method for accessing the bond connectivity patterns in molecules.

Some other modes, most notably those at 1402 and 1470 cm^{-1}, do not show the additivity; the arrival times indicate their closeness to both ends of the molecule (Figure 11), suggesting their delocalization. The atom displacement pattern for the normal mode at 1402 cm^{-1}, predicted by DFT calculations, confirms its delocalized nature (Figure 12). The ovals in Figure 11 show qualitatively the delocalization sizes for the respective modes as they appear from the RA 2DIR data. It is

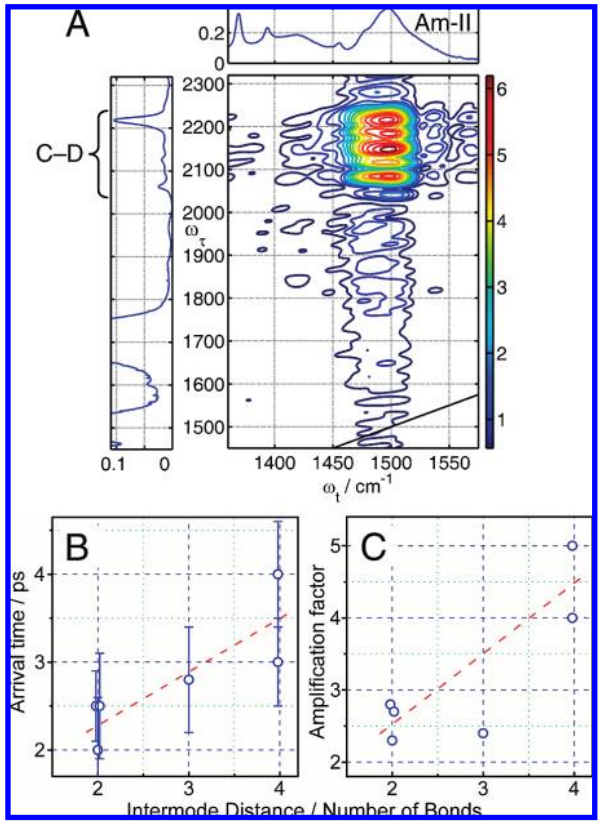

FIGURE 13. (A) Dual-frequency 2DIR rephasing spectrum of Leu-d_{10}-Boc measured at $T = 0.3$ ps with zzxx polarizations focusing on the (CD, Am-II) cross-peaks.[26,27] (B) Arrival times and (C) amplification factors measured for different CD/Am-II cross-peaks. The red dashed lines serve as a guide to the eye.

well-known that the extent of mode delocalization strongly depends upon the molecular structure.[34] Therefore, the ability of RA 2DIR to measure delocalization sizes does not only provide access to an important molecular characteristic but may lead to a new type of reporter for structural measurements. Note that the simplicity of the described analysis is dictated by a complex nature of the energy transport process, which shows the features of energy transport in macroscopic objects (induction period, non-exponential rise) but requires microscopically specific description accounting for finite mode sizes and non-equilibrium character of the energy transport.

A correlation of the arrival time and γ with the intermode distance has also been demonstrated in the Leu-d_{10}-Boc peptide (Figure 13).[26,27] Figure 13A shows the cross-peaks between various C−D modes and the Am-II mode of Leu-d_{10}-Boc. The T_{max} and γ values are plotted in panels B and C of Figure 13 as a function of the number of bonds separating the groups hosting the excited and probed modes (Figure 5C). For example, the symmetric and antisymmetric stretching modes of the $C_\beta D_2$ group are taken to be two bonds apart from the Am-II mode ($C_\beta-C_\alpha-N$). Both T_{max} and γ correlate monotonically with the intermode distance. For example, both T_{max} and γ for the $C_\delta D_3$ groups are larger than those for the $C_\beta D_2$ group. A smaller amplification factor found for the mode at 2145 cm^{-1} (plotted as $C_\gamma-D$ at abscissa = 3 in panels C and D of Figure 13) is associated with the contribution from the $C_\alpha-D$ mode, which, while it has a frequency in the middle of the spectrum, was not assigned with certainty.[27] Note that the 4−5-fold amplification found for the $C_\delta D_3$/Am-II cross-peaks will be helpful in enhancing the desired features in 2DIR spectra of proteins.

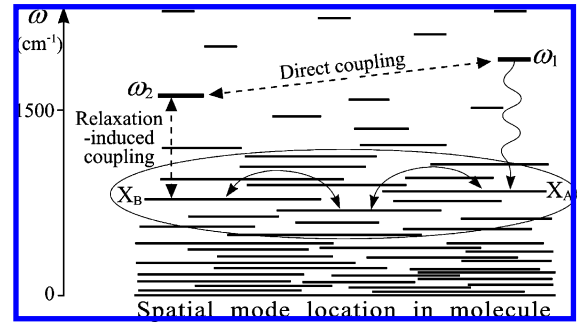

FIGURE 14. Schematic representation of fundamental vibrational states as a function of their location in a molecule. Horizontal bars show the spatial extent for vibrational modes. An initially excited ω_1 mode relaxes via the IVR process. Energy hopping between partially overlapping modes causes energy transport. Excitation of the X_B mode that spatially overlaps with the probed (ω_2) mode leads to the appearance of the relaxation-assisted cross-peaks.

Energy Transport on a Molecular Scale. Vibrational relaxation and intramolecular vibrational energy redistribution (IVR) are the core processes that determine the rate of vibrational energy flow and hence the enhancement of the cross-peaks in RA 2DIR. The diagram shown in Figure 14 helps rationalize the reasons behind the correlation of T_{max} with the distance. Two aspects are important. First, the rate of the IVR process depends upon the square of the interaction matrix element, which, in turn, depends upon the spatial overlap of the modes involved. Second, the high-frequency modes used for cross-peak measurements are (relatively) localized modes, with the delocalization size much smaller than the intermode distance. The IVR process from a localized, ω_1, mode into a largely delocalized mode(s) is not efficient because of a small overlap integral between the localized and delocalized modes. Even if such transfer occurs, the largely delocalized mode will not interact strongly with the localized ω_2 mode, again because of a small overlap, and will not contribute substantially to the RA 2DIR cross-peak. Therefore, under the given conditions, the energy hopping picture describes appropriately the energy transport process ensuring a correlation between T_{max} and the distance.

Note, that the energy transfer between the high-frequency modes accessed by IR pulses, studied experimentally[5,18,35−38] and theoretically,[39−42] is not a major mechanism contributing to the formation of relaxation-assisted cross-peaks in the systems discussed. It is the energy transport via low-frequency modes that contributes most. Energy-relaxation pathways, recently including low-frequency modes,[43] were studied by Dlott et al. using an IR pump, resonant-Raman probe method.[38] Different scenarios for vibrational energy transport could be envisioned depending upon the type of the modes excited and probed and vibrational modes present in the molecule.[44−46] For example, the energy transfer between OH, CH_2, and CH_3 stretching modes in primary alcohols, spatially separated by a single bond, accounts for only several percents of all of the deactivation pathways of the respective mode.[38] A much larger contribution (∼36%) of a single relaxation channel, the Am-I → Am-II relaxation pathway, between essentially overlapping Am-I and Am-II modes of the same amide in acetylproline-NH_2 dissolved in CH_2Cl_2 was observed,[18] indicating larger coupling. An even stronger coupling between Am-I and Am-II modes was measured[47] and computed[40] in *N*-methylacetamide in D_2O, indicated by a rapid coherent energy exchange between the modes.[47] In such a highly resonant case, the energy can propagate fast via hopping between resonant delocalized modes.[48] While it might be difficult to correlate the arrival time with the distance in the latter case, the vibrational energy can migrate to larger distances without substantial dissipation, which may enhance more the range of distances accessible via RA 2DIR studies.

5. Summary

The amplification provided by RA 2DIR, especially for spatially separated modes, is very useful for measuring weak cross-peaks. At the same time, the amplification factor serves as a structural parameter, because it can report on the intermode distance. The arrival time also correlates with distance, delivering convenient and often quickly accessible structural reporters. It remains to be seen how strongly the arrival time (or more generally, the energy transport dynamics) depends upon the three-dimensional structure of the molecule, but T_{max} is already useful in providing means for identifying overlapping transitions and testing the connectivity patterns in molecules. Note that the anisotropy of the RA 2DIR cross-peaks provides a measure of the angle between the transition dipoles of the modes exactly the same way as for the direct-coupling cross-peaks,[16] because the measured anisotropy is only sensitive to the mutual orientation of the modes accessed by radiation (polarized IR pulses), regardless of the origin of the signal (direct ω_1, ω_2 or relaxation-assisted ω_X, ω_2 coupling). Thus, the RA 2DIR cross-peak anisotropy reports on the angles between the transition dipoles and not for the modes separated by much larger distances. Further advancement of the technique requires both experimental and theoretical efforts for gaining a predictive power in correlating the energy transport time with the distance for a variety of molecular systems having different bridging structures and different frequency ranges of the two selected modes. The influence of the solvent on the vibrational relaxation and especially on the energy transport also needs to be characterized. The solvent determines the rate and amplitude of fluctuations for the energy levels in the solute, affecting both the energy transport rates in the solute and the energy dissipation to the solvent. It would be interesting to study the cross-peak amplification in the systems, where the energy transport between the two modes goes through one or several solvent molecules. We believe that establishing the rules of correlating the arrival time with the distance for a variety of bridging structures will turn RA 2DIR into an analytical method, permitting rapid measurements of connectivity patterns and intermode distances well exceeding 10−15 Å.

I am grateful to the members of my group, graduate students Gopal Naraharisetty, Valeriy Kasyanenko, Christopher Keating, and Dmitry Kurochkin, who carried out much of the work described in this Account. This work was supported in part by the Louisiana Board of Regents through Research Competitiveness Subprogram, the Enhancement Fund of Tulane University, and the National Science Foundation (Grant CHE-0750415).

BIOGRAPHICAL INFORMATION

Igor V. Rubtsov received his Ph.D. in 1992 at the Institute for Chemical Physics in Moscow. He worked at several institutions, including the Institute for Molecular Sciences, Okazaki, and the University of Pennsylvania. He is currently an Assistant Professor of Chemistry at Tulane University. His research focuses on developing methods for measuring structures and structural dynamics in biopolymers.

REFERENCES

1 Hamm, P.; Lim, M.; Hochstrasser, R. M. Structure of the amide I band of peptides measured by femtosecond non-linear infrared spectroscopy. *J. Phys. Chem. B* **1998**, *102*, 6123–6138.

2 Asplund, M. C.; Zanni, M. T.; Hochstrasser, R. M. Two-dimensional infrared spectroscopy of peptides by phase-controlled femtosecond vibrational photon echoes. *Proc. Natl. Acad. Sci. U.S.A.* **2000**, *97*, 8219–8224.

3 Mukamel, S. Multidimensional femtosecond correlation spectroscopies of electronic and vibrational excitations. *Annu. Rev. Phys. Chem.* **2000**, *51*, 691–729.

4 Zheng, J.; Kwak, K.; Asbury, J.; Chen, X.; Piletic, I. R.; Fayer, M. D. Ultrafast dynamics of solute−solvent complexation observed at thermal equilibrium in real time. *Science* **2005**, *309*, 1338–1343.

5 Kim, Y. S.; Hochstrasser, R. M. Chemical exchange 2D IR of hydrogen-bond making and breaking. *Proc. Natl. Acad. Sci. U.S.A.* **2005**, *102*, 11185–11190.

6 Hamm, P.; Helbing, J.; Bredenbeck, J. Two-dimensional infrared spectroscopy of photoswitchable peptides. *Annu. Rev. Phys. Chem.* **2008**, *59*, 291–317.

7 Chung, H. S.; Ganim, Z.; Jones, K. C.; Tokmakoff, A. Transient two-dimensional IR spectroscopy of ubiquitin unfolding dynamics. *Proc. Natl. Acad. Sci. U.S.A.* **2007**, *104* (36), 14237–14242.

8 Demirdoeven, N.; Cheatum, C. M.; Chung, H. S.; Khalil, M.; Knoester, J.; Tokmakoff, A. Two-dimensional infrared spectroscopy of antiparallel β-sheet secondary structure. *J. Am. Chem. Soc.* **2004**, *126*, 7981–7990.

9 Fang, C.; Senes, A.; Cristian, L.; DeGrado, W. F.; Hochstrasser, R. M. Amide vibrations are delocalized across the hydrophobic interface of a transmembrane helix dimer. *Proc. Natl. Acad. Sci. U.S.A.* **2006**, *103*, 16740–16745.

10 Asbury, J. B.; Steinel, T.; Fayer, M. D. Vibrational echo correlation spectroscopy probes of hydrogen bond dynamics in water and methanol. *J. Lumin.* **2004**, *107*, 271–286.

11 Kraemer, D.; Cowan, M. L.; Paarmann, A.; Huse, N.; Nibbering, E. T. J.; Elsaesser, T.; Miller, R. J. D. Temperature dependence of the two-dimensional infrared spectrum of liquid H_2O. *Proc. Natl. Acad. Sci. U.S.A.* **2008**, *105*, 437–442.

12 Hochstrasser, R. M. Two-dimensional spectroscopy at infrared and optical frequencies. *Proc. Natl. Acad. Sci. U.S.A.* **2007**, *104*, 14190–14196.

13 Dreyer, J.; Moran, A. M.; Mukamel, S. Coherent three-pulse spectroscopy of coupled vibrations in a rigid dipeptide: Density functional theory simulations. *J. Phys. Chem. B* **2003**, *107*, 5967–5985.

14 Rubtsov, I. V.; Wang, J.; Hochstrasser, R. M. Dual frequency 2D-IR heterodyned photon-echo of the peptide bond. *Proc. Natl. Acad. Sci. U.S.A.* **2003**, *100*, 5601–5606.

15 Kurochkin, D. V.; Naraharisetty, S. R. G.; Rubtsov, I. V. Relaxation-assisted 2D IR using weak vibrational modes. *Springer Ser. Chem. Phys.* **2007**, *88*, 344–346.

16 Kurochkin, D. V.; Naraharisetty, S. G.; Rubtsov, I. V. Relaxation-assisted 2D IR spectroscopy method. *Proc. Natl. Acad. Sci. U.S.A.* **2007**, *104*, 14209–14214.

17 Hamm, P.; Hochstrasser, R. M. In *Ultrafast Infrared and Raman Spectroscopy*; Fayer, M. D., Ed.; Marcel Dekker, Inc.: New York, 2000; p 273.

18 Rubtsov, I. V.; Hochstrasser, R. M. Vibrational dynamics, mode coupling and structure constraints for acetylproline−NH_2. *J. Phys. Chem. B* **2002**, *106*, 9165–9171.

19 Rubtsov, I. V.; Kumar, K.; Hochstrasser, R. M. Dual-frequency 2D IR photon echo of a hydrogen bond. *Chem. Phys. Lett.* **2005**, *402*, 439–443.

20 Kurochkin, D. V.; Naraharisetty, S. G.; Rubtsov, I. V. Dual-frequency 2D IR on interaction of weak and strong IR modes. *J. Phys. Chem. A* **2005**, *109*, 10799–10802.

21 Fang, C.; Hochstrasser, R. M. Two-dimensional infrared spectra of the ^{13}C:^{18}O isotopomers of alanine residues in an α-helix. *J. Phys. Chem. B* **2005**, *109*, 18652–18663.

22 Rubtsov, I. V.; Wang, J.; Hochstrasser, R. M. Vibrational coupling between amide-I and amide-A modes revealed by femtosecond two-color infrared spectroscopy. *J. Phys. Chem. A* **2003**, *107*, 3384–3396.

23 Sagle, L. B.; Zimmermann, J.; Matsuda, S.; Dawson, P. E.; Romesberg, F. E. Redox-coupled dynamics and folding in cytochrome *c*. *J. Am. Chem. Soc.* **2006**, *128*, 7909–7915.

24 Naraharisetty, S. G.; Kurochkin, D. V.; Rubtsov, I. V. C−D modes as structural reporters via dual-frequency 2DIR spectroscopy. *Chem. Phys. Lett.* **2007**, *437*, 262–266.

25 Ha, J.-H.; Kim, Y. S.; Hochstrasser, R. M. Vibrational dynamics of N−H, C−D, and C═O modes in formamide. *J. Chem. Phys.* **2006**, *124*, 064508/1-10.

26 Naraharisetty, S. G.; Kasyanenko, V. M.; Zimmermann, J.; Thielges, M.; Romesberg, F. E.; Rubtsov, I. V. In *Springer Series in Chemical Physics*; Corkum, P. B., De Silvestri, S., Nelson, K. A., Eds.; Springer: Berlin, Germany, 2009; Vol. 92.

27 Naraharisetty, S. R. G.; Kasyanenko, V. M.; Zimmermann, J.; Thielges, M. C.; Romesberg, F. E.; Rubtsov, I. V. C−D modes of deuterated side chain of leucine as structural reporters via dual-frequency two-dimensional infrared spectroscopy. *J. Phys. Chem. B* **2009**, *113*, 4940–4946.

28 Fang, C.; Baumann, J. D.; Das, K.; Remorino, A.; Arnold, E.; Hochstrasser, R. M. Two-dimensional infrared spectra reveal relaxation of the nonnucleoside inhibitor TMC278 complexed with HIV-1 reverse transcriptase. *Proc. Natl. Acad. Sci. U.S.A.* **2008**, *105*, 1472–1477.

29 Kozinski, M.; Garrett-Roe, S.; Hamm, P. 2D-IR spectroscopy of the sulfhydryl band of cysteines in the hydrophobic core of proteins. *J. Phys. Chem. B* **2008**, *112*, 7645–7650.

30 Lim, M.; Hamm, P.; Hochstrasser, R. M. Protein fluctuations are sensed by stimulated infrared echoes of the vibrations of carbon monoxide and azide probes. *Proc. Natl. Acad. Sci. U.S.A.* **1998**, *95*, 15315–15320.

31 Rubtsov, I. V.; Naraharisetty, S. R. G.; Kasyanenko, V. M.; Keating, C. S. In 235th American Chemical Society (ACS) National Meeting in New Orleans, LA, 2008; PHYS-116.

32 Naraharisetty, S. G.; Kasyanenko, V. M.; Rubtsov, I. V. Bond connectivity measured via relaxation-assisted two-dimensional infrared spectroscopy. *J. Chem. Phys.* **2008**, *128*, 104502–104507.

33 Golonzka, O.; Khalil, M.; Demirdoven, N.; Tokmakoff, A. Vibrational anharmonicities revealed by coherent two-dimensional infrared spectroscopy. *Phys. Rev. Lett.* **2001**, *86*, 2154–2157.

34 Torii, H.; Tasumi, M. Model calculations on the amide-I infrared bands of globular proteins. *J. Chem. Phys.* **1992**, *96*, 3379–3387.

35 Woutersen, S.; Mu, Y.; Stock, G.; Hamm, P. Subpicosecond conformational dynamics of small peptides probed by two-dimensional vibrational spectroscopy. *Proc. Natl. Acad. Sci. U.S.A.* **2001**, *98*, 11254–11258.

36 Khalil, M.; Demirdoven, N.; Tokmakoff, A. Vibrational coherence transfer characterized with Fourier-transform 2D IR spectroscopy. *J. Chem. Phys.* **2004**, *121*, 362–373.

37 Nibbering, E. T. J.; Elsaesser, T. Ultrafast vibrational dynamics of hydrogen bonds in the condensed phase. *Chem. Rev.* **2004**, *104*, 1887–1914.

38 Wang, Z.; Pakoulev, A.; Dlott, D. D. Watching vibrational energy transfer in liquids with atomic spatial resolution. *Science* **2002**, *296*, 2201–2203.

39 Mukamel, S. Non-Markovian theory of molecular relaxation. I. Vibrational relaxation and dephasing in condensed phases. *Chem. Phys.* **1979**, *37*, 33–47.

40 Bloem, R.; Dijkstra, A. G.; Jansen, T. L.; Knoester, J. Simulation of vibrational energy transfer in two-dimensional infrared spectroscopy of amide I and amide II modes in solution. *J. Chem. Phys.* **2008**, *129*, 055101/1-9.

41 Jansen, T. L.; Knoester, J. Two-dimensional infrared population transfer spectroscopy for enhancing structural markers of proteins. *Biophys. J.* **2008**, *94*, 1818–1825.

42 Deng, Y.; Stratt, M. Vibrational eenrgy relaxation of polyatomic molecules in liquids: The solvent's perspective. *J. Chem. Phys.* **2002**, *117*, 1735–1749.

43 Seong, N.-H.; Fang, Y.; Dlott, D. D. Vibrational energy dynamics of normal and deuterated liquid benzene. *J. Phys. Chem. A* **2009**, *113*, 1445–1452.

44 Fujisaki, H.; Straub, J. E. Vibrational energy relaxation in proteins. *Proc. Natl. Acad. Sci. U.S.A.* **2005**, *102*, 6726–6731.

45 Gruebele, M.; Wolynes, P. G. Vibrational energy flow and chemical reactions. *Acc. Chem. Res.* **2004**, *37*, 261–267.

46 Leitner, D. M. Heat transport in molecules and reaction kinetics: the role of quantum energy flow and localization. *Adv. Chem. Phys.* **2005**, *130 B*, 205–256.

47 DeFlores, L. P.; Ganim, Z.; Ackley, S. F.; Chung, H. S.; Tokmakoff, A. The anharmonic vibrational potential and relaxation pathways of the amide I and II modes of *N*-methylacetamide. *J. Phys. Chem. B* **2006**, *110*, 18973–18980.

48 Backus, E. H. G.; Nguyen, P. H.; Botan, V.; Moretto, A.; Crisma, M.; Toniolo, C.; Zerbe, O.; Stock, G.; Hamm, P. Structural flexibility of a helical peptide regulates vibrational energy transport properties. *J. Phys. Chem. B* **2008**, *112*, 15487–15492.